Applied Radiation and Isotopes 96 (2015) 139–147

Contents lists available at ScienceDirect

Applied Radiation and Isotopes

journal homepage: www.elsevier.com/locate/apradiso

Continuous versus pulse neutron induced gamma spectroscopy for soil carbon analysis

A. Kavetskiy, G. Yakubova, H.A. Torbert *, S.A. Prior

USDA-ARS National Soil Dynamics Laboratory, 411 South Donahue Drive, Auburn, AL 36832, USA

HIGHLIGHTS

- Calibration of the neutron induced gamma analysis system must account for system background and the interference of other nuclei (mainly silicon-28) on the carbon peak at 4.43 MeV.
- Spectra measured at a height of 250 cm above the ground could be considered the NGA system background spectrum.
- The experimental cascade transition coefficient for silicon-28 (i.e. ratio of 4.50–1.78 MeV gamma ray intensities) agrees well with theoretical calculations.
- The NGA continuous working mode halved the measurement time compared to the pulse working mode while retaining the same degree of accuracy.

ARTICLE INFO

Article history:
Received 14 May 2014
Received in revised form
30 July 2014
Accepted 29 October 2014
Available online 20 November 2014

Keywords:
Soil carbon
Soil analysis
Inelastic neutron scattering
Thermo neutron capture
Neutron generator

ABSTRACT

Neutron induced gamma spectra analysis (NGA) provides a means of measuring carbon in large soil volumes without destructive sampling. Calibration of the NGA system must account for system background and the interference of other nuclei on the carbon peak at 4.43 MeV. Accounting for these factors produced measurements in agreement with theoretical considerations. The continuous NGA mode was twice as fast and just as accurate as the pulse mode, thus this mode was preferable for routine soil carbon analysis.

Published by Elsevier Ltd.

1. Introduction

An emerging method for soil carbon analysis in the field is the measurement of gamma rays from soils subjected to neutron irradiation. There are different processes of neutron interaction with nuclei that produce gamma rays; measurement of this irradiation can be used to determine soil elements. For example, the inelastic neutron scattering (INS) of fast neutrons (~14 MeV) from carbon-12 nuclei produce gamma rays (4.43 MeV) that can be used to determine soil carbon (Wielopolski, 2011). Neutron induced gamma spectra analysis (NGA) has several advantages over other methods of carbon determination such as dry combustion, mid and near infrared reflectance spectroscopy, and laser induced breakdown spectroscopy. The NGA method is a non-destructive method that requires no sample preparation and is capable of analyzing large volumes of soil at once (Wielopolski, 2011). But determining the number of counts from gamma rays with energy of 4.43 MeV attributed to carbon is challenging using this method since several other nuclei and processes contribute to this peak in the gamma spectra. For example, some gamma rays that overlap this area are generated from neutron interactions with silicon-28 nuclei (Wielopolski, 2011; Basunia, 2013); silicon is one of the main components of soil. Other nuclei (i.e. aluminum-27, oxygen-16) under neutron irradiation can also contribute to this range of interest.

Neutron generation and gamma spectra acquisition can be performed in two modes: continuous and pulse. In the continuous mode, a single gamma spectrum encompassing INS processes, thermal neutron capture (TNC), delay neutron activation, and natural background is acquired. In the pulse mode, separate gamma spectra are acquired during and between neutron pulses. The gamma spectrum acquired during the pulse is similar to the continuous mode spectrum. The gamma spectrum acquired between pulses is attributed to TNC, delay neutron activation, and

* Corresponding author.
E-mail address: allen.torbert@ars.usda.gov (H.A. Torbert).

http://dx.doi.org/10.1016/j.apradiso.2014.10.024
0969-8043/Published by Elsevier Ltd.

natural background; it is free from INS gamma rays. Gamma spectra acquisition during and between neutron pulses has an advantage over the continuous regime since it allows for more elaborate analysis of different elements and processes that are responsible for peaks in the spectra. However, in this mode the neutron irradiation intensity during the pulse depends on the duty cycle and frequency of the neutron generator setup (total number of neutron in unit time is constant) which is higher than the continuous mode. The disadvantages of the pulse mode occur at higher neutron fluxes where the background level is higher (increased pile-up overlapping in range of interest by low energy gammas), areas of peaks of interest are less (due to increasing dead time), so the signal-to-noise ratio in the range of interest is less, and relative error is higher.

An in-depth evaluation of measurement modes and subsequent data processing procedures for efficiently and accurately surveying soil carbon will be discussed. The mode most suitable for routine field measurement of soil carbon will be identified.

2. Materials and methods

The NGA measurement system for soil carbon analysis consists of a neutron generator, gamma detector, protective shielding, and construction materials (Wielopolski, 2011). A neutron generator (Model MP320; ThermoScientific, Waltham, MA) suitable for this method produces fast neutrons with energy of 14 MeV due to the nuclear reaction of tritium and deuterium. A neutron flux equal to $\sim 10^8$ neutron s^{-1} can be produced by this generator in the continuous or pulse modes with a frequency of 1–25 kHz and a duty cycle of 5–100% (100% duty cycle corresponds to the continuous or direct current (DC) mode of measurement). The cross section of inelastic neutron scattering on carbon-12 nuclei, leading to the production of 4.43 MeV gamma rays, is relatively large (0.21 barns for 14 MeV neutrons; MacFarlane, 2014). One or several NaI (Tl) detectors with individual operating volumes of $\sim 2500\ cm^3$ were used for gamma ray detection. For data acquisition, split electronics with corresponding ProSpect v0.1.11-vega software (XIA LLC, Hayward, CA) allowed for acquiring either a single spectrum (continuous mode) or two spectra during and between pulses simultaneously (pulse mode). IGOR software was used for gamma-spectra analysis (WaveMetrics, 2013). It should be noted that the NaI(Tl) detector volume is more than adequate for full adsorption of gamma rays untill energy of 8–10 MeV (Saint-Gobain Crystals, 2009). The first approximation of adsorption efficiency for such a large crystal (12.5 cm × 12.5 cm × 15.2 cm) practically does not change with energy. According to Monte-Carlo calculations (Saint-Gobain Crystals, 2009), the "peak-to-total" ratio in the main range of interest (from 1.8 to 4.5 MeV) for the large crystal does not change significantly. For these reasons, the spectra correction based on the dependence of the efficiency of gamma-ray registration with energy (product of adsorption efficiency on the "peak-to-total" ratio) was not considered in this research.

Since soil carbon concentration is typically quite low, the useful signal (net peak area with centroid at 4.43 MeV) is only slightly higher than background (Wielopolski et al., 2008a); therefore, to accurately determine such a low useful signal, identifying all components in the peaks of interest (inclusive of background spectra) and implementing correct data processing is very important.

A critical step is to determine the NGA system background which is the spectrum radiated by the construction material under neutron irradiation. System background is always present and can be determined by raising the NGA system until the signal is unaffected by the ground or other large objects. In this study, the NGA system equipped with one gamma-detector was raised to various heights over a sand substrate to determine at what height the sand substrate no longer affected the measured spectra.

A Monte Carlo simulation was undertaken to better understand the behavior of neutron simulated gamma spectra with changing height. A sodium iodide detector having a similar geometry to our measurement system (i.e., detector size, disposition of neutron source and detector, and size of aluminum shield between neutron source and detector) was used in conjunction with a Geant4 toolkit (Agostinelli et al., 2003). The gamma spectra were compared to gamma lines simulated by the Geant4 toolkit and G4NDL4.0 neutron database to identify the nuclei responsible for peaks of interest (Geant4, 2014).

Another critical step is to determine the portion of the 4.43 MeV peak contributed by silicon-28 interference. The cascade transition coefficient value that accounts for this interference was calculated from spectra measured from silicon samples with different layer thicknesses. The silicon samples (bulk density 1.26 g cm^{-3}) were prepared using granulated silicon placed in stainless steel boxes (40 cm × 40 cm × H where H varied from 1 to 20 cm). Boxed samples were attached to the NGA system and raised to a height of 260 cm prior to measurement.

Understanding the dependence of the carbon peak area in the neutron stimulated gamma-spectra versus the carbon concentration in the sample is important for calibration purposes. For NGA system calibration, mixtures of sand with granulated carbon were prepared, and subsequent measurements were carried out. The mixtures were prepared by mechanical mixing (manually or concrete mixer) sand with a specified amount of granulated coconut shells (~1.5 mm diameter; 100% carbon content) until uniformity was attained. Six samples with 1, 2.5, 5, 7.5, 10 and 15% carbon by weight ($Cw\%$) were prepared. The bulk density of the mixture (d_{mix}, g cm^{-3}) with changing $Cw\%$ was described as follows:

$$d_{mix} = \frac{1.7 \times 0.52 \times 100}{Cw\%1.7 + (100 - Cw\%)0.52} \quad (1)$$

where 1.7 is bulk density of sand, g cm^{-3}; 0.52 is bulk density of coconut shells, g cm^{-3}.

Each sample mixture was placed in a stainless steel box (40 cm × 40 cm × 20 cm) and was attached to the NGA system; both were raised to a height of 260 cm prior to measurement.

Soil was also collected from an experimental soil bin located at the National Soil Dynamics Laboratory in Auburn, AL (Batchelor, 1984) to test the accuracy of the NGA measurements in both regimes. The selected soil was a Houston clay (very-fine, smectitic, thermic Oxyaquic Hapluderts) which had a relatively high carbon concentration (i.e., ~2.8). A sample was prepared by mixing ~5 w % additional granulated carbon for measurement via the NGA system. In addition, subsamples were collected from soil and sample mixtures, ground with a roller grinder (Kelley, 1994), and analyzed by dry combustion method utilizing a LECO TruSpec CN analyzer (LECO Corp., Saint Joseph, MI) for comparison.

3. Results and discussion

3.1. Measurement of system background

The background or portion of the spectra radiated by construction material was determined. Accounting for this background is critical since the carbon signal is only slightly higher than background (Wielopolski et al., 2008a) and thus is important for correcting all data. In this study, the NGA system equipped with one gamma-detector was raised to increasing heights over a sand substrate to determine at what height the signal was unaffected by the ground surface or other large objects.

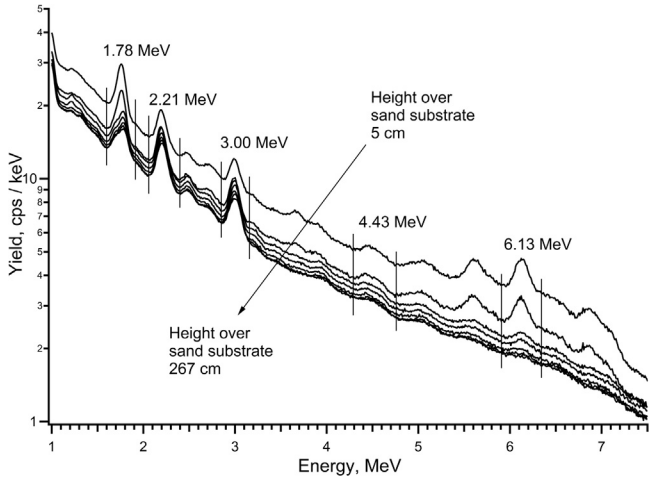

Fig. 1. Experimental gamma-spectra at different placement heights of the NGA system over a sand substrate.

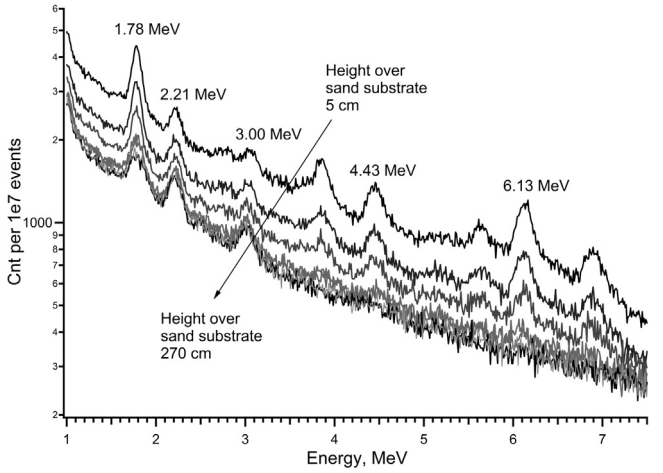

Fig. 3. Geant4 simulated gamma-spectra at different placement heights of the NGA system over a sand substrate.

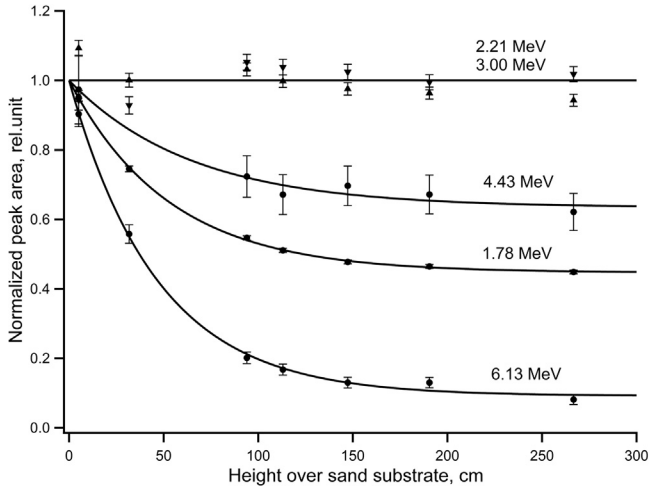

Fig. 2. Dependence of normalized main peaks areas in the experimental gamma-spectra (points with error bars) to changing heights above a sand substrate (lines are approximations).

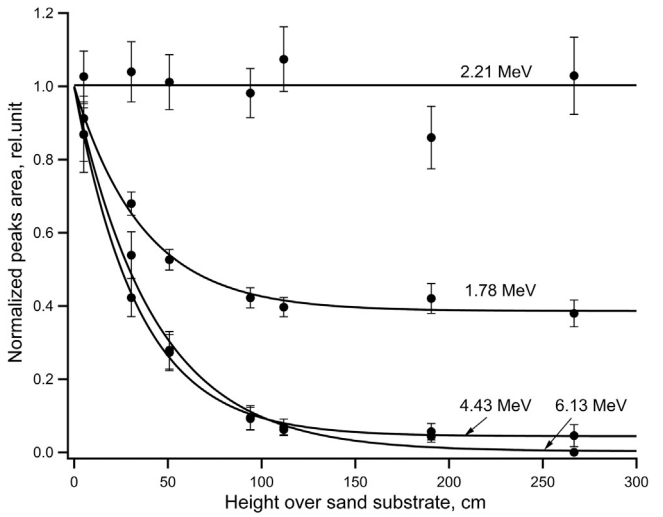

Fig. 4. Dependence of normalized main peaks areas in the simulated gamma-spectra (points with error bars) to changing heights above a sand substrate (lines are approximations).

The height results of measurements of a neutron stimulated gamma-spectra taken in the DC regime are shown in Fig. 1. Peak areas and respective standard deviations were calculated according to procedures described by Gilmore (2008). The experimental dependences of normalized main peaks areas in the gamma spectra to changing height are shown in Fig. 2 by points with error bars at a confidence level of 0.68 (here and all following error calculations). Based on these observations, the transformations of the gamma spectra with increasing height leads to the following conclusions:

- the background level continually decreased;
- some peak areas exhibited little change with height (2.21 MeV, 3.00 MeV peaks);
- some peak areas decreased and reached a constant level at height >250 cm (1.78 MeV, 4.43 MeV, 6.13 MeV peaks).

Using a simulation system with similar geometry to our system (i.e., detector type, size, disposition of neutron source and detector, and size of aluminum shield between neutron source and detector) and the Geant4 toolkit with the G4NDL4.0 worldwide neutron database (which contain the cross-section for neutron interaction processes), a Monte Carlo simulation of gamma spectra over a sand substrate was done to better characterize gamma spectra with changing height. Results of spectra simulations are presented in Fig. 3, and the dependencies of main peak areas with height are presented in Fig. 4. Comparison of Fig. 1 with Fig. 3 and Fig. 2 with Fig. 4 demonstrated that the simulated spectra had many common features relative to experimental results.

The analysis of experimental and simulated gamma spectra under neutron irradiation at different heights over sand substrate leads to a number of conclusions.

- Spectral changes are negligible over a height of 250 cm suggesting little neutron interaction with substrate nuclei at greater heights. It is important to note that simulated spectra at heights >250 cm are identical to simulated spectra in the absence of sand substrate. Spectra measured at heights above 250 cm could be considered the NGA system background spectrum.
- Two peaks of interest in the NGA system background spectrum from the point of view of carbon measurement are those with centroids at 4.43 MeV and 1.78 MeV. The peak at 4.43 MeV is the background for carbon while the 1.78 MeV peak is the background for silicon; how the silicon peak is used for

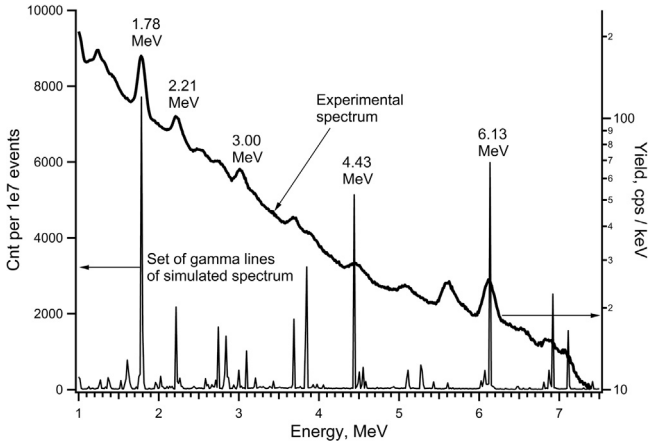

Fig. 5. Sand spectrum measured at 5 cm height and set of silicon dioxide gamma lines simulated by Geant4.

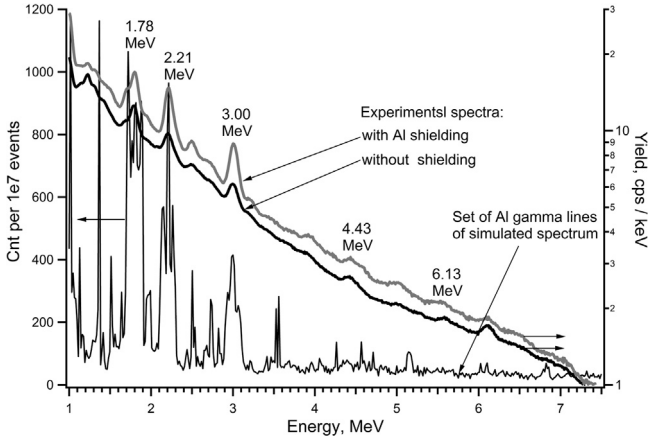

Fig. 6. The NGA system background spectrum at 260 cm height and set of aluminum gamma lines simulated by Geant4.

correcting the carbon 4.43 MeV peak will be discussed later.

To identify the nuclei responsible for different peaks of interest, the experimental gamma spectra were compared to a set of gamma lines simulated by the Geant4 toolkit with the G4NDL4.0 neutron database. A comparison of sand spectrum measured at a height of 5 cm to a set of simulated silicon dioxide gamma lines (e.g., Hadr03 from Geant4 toolkit) is shown in Fig. 5. This comparison shows that some peaks in the measured spectra can be produced by silicon dioxide. For example, peaks at 1.78 MeV are produced by the silicon-28 nuclei while peaks at 6.13 MeV are due to the oxygen-16 nuclei, etc. At least a portion of the 4.43 MeV peak can be attributed to the oxygen-16 nuclei. Some peaks are absent in the simulated set, for example, the peak around 3.0 MeV. The NGA system background spectrum versus the simulated aluminum spectrum is shown in Fig. 6. The peaks with centroids at 1.78, 2.21, and 3.00 MeV could be produced by aluminum-27 nuclei from the experimental protective shielding. Removing the protective aluminum shielding reduced but did not totally eliminate these peaks; other possible sources might be aluminum in the tube and electronic block bodies of the neutron generator. Since the peak at 4.43 MeV in the NGA background spectra did not changed with shielding removal, this probably represents oxygen in the air (we have the 4.43 MeV gamma line in the oxygen simulated spectrum set). Collectively, these finding indicated that the NGA system background peaks should be subtracted from the measured peaks in the determination of soil carbon.

Previously the origin of gamma spectra peaks acquired during pulses in the pulse mode (INS spectra) or continuous mode (DC spectra) was discussed. The gamma spectra acquired between pulses is due to TNC processes, delay neutron activation, and natural background (i.e., TNC spectra; Wielopolski et al., 2008b). There are several gamma peaks in the TNC spectrum measured at heights greater than 250 cm above the substrate (NGA system background spectra) including the peak with energy 1.78 MeV. Database (Sonzogni, 2014) analysis discloses that among nuclei present in the measurement system vicinity of 250 cm, beta-decay of aluminum-28 nuclei can give rise to this gamma line. Aluminum-28 can result from the thermal neutron capture by aluminum-27 (isotope with a natural abundance 100%; Gray, 2013). In the immediate vicinity of the neutron source there is an aluminum tube, the neutron generator body, and the aluminum body of the gamma detector. Induced activity of aluminum (due to interactions with thermal neutrons) can be attributed to these equipment parts. The number of nuclei N (aluminum-28) due to neutron irradiation will accumulate over time t according to Eq. (2) (Turner, 2007)

$$N(t) = \frac{A}{\lambda}(1 - e^{-\lambda t}) \tag{2}$$

where A is a constant term proportional to the intensity of irradiation and the number of target nuclei, and λ is an aluminum-28 decay constant (λ=0.005156 s^{-1}, decay time $T_{1/2} = \frac{\ln(2)}{\lambda} = 2.24$ min; Sonzogni, 2014). The peak area S with centroid at 1.78 MeV in the TNC system background spectrum with time τ will follow the Eq. (3):

$$S(\tau) \sim \int_0^{\tau} \lambda N(t)dt = \frac{A}{\lambda}(\lambda\tau + e^{-\lambda\tau} - 1) \tag{3}$$

For determining the experimental dependence of the peak area with centroid at 1.78 MeV over time, several snapshots were recorded during the measurement of the TNC system background spectrum (Fig. 7). The position of some peaks inclusive of the 1.78 MeV peak are identified in this figure. The 1.78 MeV peak area and standard deviation were calculated according to standard procedures described elsewhere (Gilmore, 2008). The increase in peak area with a centroid of 1.78 MeV over time is shown in Fig. 8 by points; Eq. (3) was used to characterize this dependence. As can be seen, the fitted line is in full agreement with experimental observations (within the experimental error) for all measurement times (3–4000 s). This indicates that the thermal neutron activation of aluminum controls the peak at 1.78 MeV in TNC system background spectrum. It should be noted that these gamma rays also exist in the INS spectra, because they are present

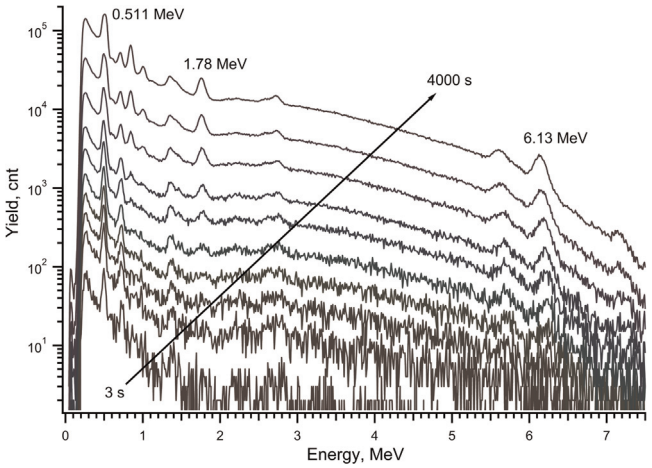

Fig. 7. Snapshots of the NGA system background TNC spectra.

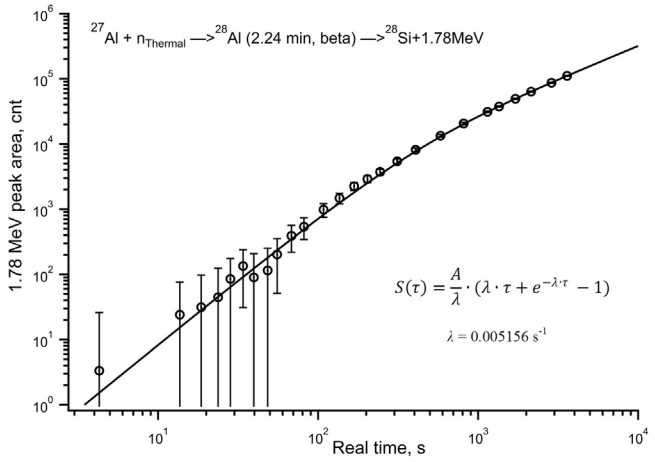

Fig. 8. Dependence of 1.78 MeV peak areas in the NGA system background TNC spectra with irradiation time.

continuously, not only out of neutron pulse. The 1.78 MeV peaks in NGA system background overlap the 1.78 MeV peak spectra of soil samples. Thus, the 1.78 MeV peak areas in NGA system background spectra need to be accounted for in the calculation of 1.78 MeV peak areas in the TNC and INS spectra associated with silicon during soil measurements.

3.2. Accounting for silicon-28 interference

The peak with a centroid of 4.43 MeV can be used for determination of carbon contained in soil. However, gamma rays from other soil elements and processes overlap this area. In this regard, silicon-28 gamma lines need to be taken into account (Wielopolski, 2011). The decay of silicon in the excited state (6.28 MeV), which appear under interaction with fast neutrons, to the ground state occurs via cascade feeding the 1.78 MeV-level. A fraction of this cascade generates 4.50 MeV (i.e., difference between 6.28 and 1.78) gamma rays that overlap the 4.43 MeV carbon peak. For silicon-28, the ratio of 4.50–1.78 MeV gamma ray intensities is constant and equal to 0.0547 according to theoretical calculations by the EMPIRE code (Wielopolski et al., 2008b; Herman et al., 2007). This ratio can be experimentally estimated from the INS and TNC silicon gamma spectra by calculating the fraction of the 1.78 and 4.50 MeV INS peaks that are associated only with silicon. For this purpose, the INS and TNC spectra from the silicon samples (40 cm × 40 cm × H where H varied from 1 to 20 cm) under neutron irradiation were taken. The measurements were conducted at a 260 cm height and far from the walls where the spectral effects of the sand substrate and concrete walls were negligible (Fig. 9). The INS and TNC for the NGA system background spectra at pulse operation regime are also shown in Fig. 9.

Based on these results the following should be noted:

1) Gamma rays with energy around 1.78 MeV which contribute to the 1.78 MeV peak in the INS spectra can result in the irradiation of the silicon sample by fast neutrons due to
   a) direct transition from 1.78 MeV level to ground state in silicon-28 excited by fast neutrons (including cascade transition of higher excited levels passing through the 1.78 MeV level)
   b) decay of aluminum-28 produced by the ^{28}Si(n, p)^{28}Al reaction; and
   c) system background likely due to both inelastic neutron scattering on aluminum-27 and aluminum-28 decay ($T_{1/2}$ = 2.24 min, ε_γ = 1.78 MeV) produced from the ^{27}Al + n$_{thermal}$ → ^{28}Al reaction in aluminum parts of equipment (system background).
2) Gamma rays with energy around 1.78 MeV which contribute to the 1.78 MeV peak in the TNC spectra can result in the irradiation of the silicon sample by fast neutrons due to
   a) decay of aluminum-28 produced by the ^{28}Si (n, p)^{28}Al reaction; and
   b) decay of aluminum-28 from the ^{27}Al + n$_{thermal}$ → ^{28}Al reaction of aluminum parts of equipment (system background).
3) Gamma rays with energy around 4.43–4.50 MeV which contribute to the 4.43 MeV peak in the INS spectra can result in the irradiation of the silicon sample by fast neutrons due to
   a) cascade transition from 6.28 MeV to 1.78 MeV level for silicon-28 excited by fast neutrons; and
   b) unidentified 4.43 peak in the background spectra (possibly oxygen in the atmosphere).
4) No peaks were noted in the area around 4.43 MeV in the TNC spectra of silicon samples and the NGA system background when the neutron generator's working regime was at a 5 kHz frequency, 25% duty cycle, 0 μs delay time, and 2 μs extension time. A peak with centroid at 4.95 MeV and its single escape peak at 4.43 MeV can appear in TNC spectra due to thermal neutron capture of silicon-28 nuclei from silicon or sand (Wielopolski et al., 2008b). However, these peaks were not observed possibly due to our sample volumes not being sufficient enough for neutron thermalization and stimulation of this reaction.

The total real time (RT) of spectra acquisition was 1 h. The live time (LT) for INS and TNC spectra were different because of the neutron generator pulse working regime; this varied for each spectrum in relation to different gamma-detector dead time due to changing gamma flux intensities from different samples. Thus, different spectra were compared by count rate (i.e. counts divided by live time); and areas for peaks of interest (Fig. 9 at enlarge scale) were calculated using standard procedures (Gilmore, 2008) in counts per second (cps). Taking the above into account, it is possible to determine the following:

1) The fraction of the 1.78 MeV peak in the INS spectrum that is related to the transition from the 1.78 MeV excited level to ground state for silicon-28 ($S_{Si1.78\text{-}GS,INS}$, cps) is given by

$$S_{Si1.78-GS,INS} = (S_{Si1.78,INS} - S_{Bkg1.78,INS}) - (S_{Si1.78,TNC} - S_{Bkg1.78,TNC}) \quad (4)$$

   where $S_{Si1.78,INS}$ is a peak area with centroid at 1.78 MeV in the INS silicon spectrum (cps), $S_{Bkg1.78,INS}$ is a peak area with centroid at 1.78 MeV in the INS background spectrum (cps), $S_{Si1.78,TNC}$ is a peak area with centroid at 1.78 MeV in the TNC silicon spectra (cps), $S_{Bkg1.78,TNC}$ is a peak area with centroid at 1.78 MeV in the TNC background spectra (cps); and
2) The fraction of the 4.50 MeV peak in the INS spectrum that is related to the cascade transition from 6.28 MeV level to 1.78 MeV level for silicon-28 $S_{SiCAS4.43,INS}$, cps) is given by

$$S_{SiCAS4.50,\ INS} = S_{Si4.50,INS} - S_{Bkg4.50,INS} \quad (5)$$

where $S_{Si4.50,INS}$ is a peak area with centroid at 4.50 MeV in the INS silicon spectrum (cps), $S_{Bkg4.50,INS}$ is a peak area with centroid at 4.50 MeV in the INS background spectrum (cps).

According to Eqs. (4) and (5), the fraction of the peak area with energy of 4.50 MeV that is related to the cascade transition from 6.28 MeV level to 1.78 MeV level, and the fraction of the peak area with energy of 1.78 MeV related to transition from 1.78 MeV level

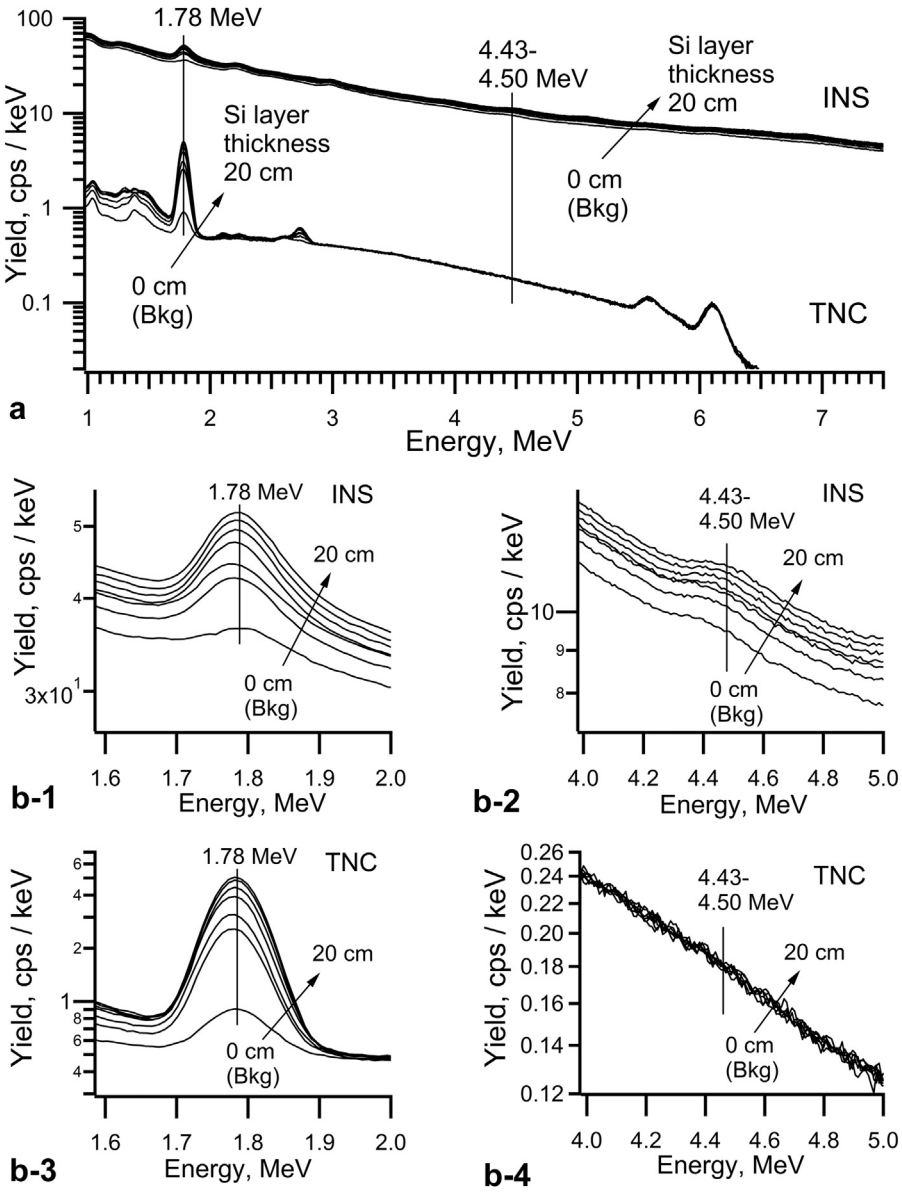

Fig. 9. INS and TNC of the NGA system spectra under 14 MeV neutron irradiation for background and samples of granulated Si (bulk density d = 1.26 g cm^{-3}) sized 40 cm × 40 cm with different layer thickness (1–20 cm) (a); range of interest at an enlarged scale (b1–b4).

to ground state for silicon-28 were calculated from the measured spectra (Fig. 9). The dependence of $S_{SiCAS4.50,INS}$ versus $S_{Si1.78-GS,INS}$ is shown in Fig. 10 by points with error bars; the fitting of this data is a straight line with a slope of 0.056 passing through the origin (solid line). Despite relatively large standard deviations, this slope agrees well with the theoretically calculated ratio of 0.0547 (i.e., 4.50 to 1.78 MeV transitions in excited silicon-28). Thus it is possible to conclude that the above described algorithm for determining a correlation between the 1.78 and 4.43 MeV peak areas is correct. It should be noted that the dependence of $S'_{Si1.78-GS,INS}$ to $S'_{SiCAS4.50,INS}$, where $S'_{Si1.78-GS,INS} = S_{Si1.78INS} - S_{Si1.78TNC}$ and $S'_{SiCAS4.50,INS} = S_{Si4.50INS}$ (i.e. without accounting for background spectra), gives a straight line fitting which does not pass through the origin and has a slope twice that of the theoretical calculation.

The contribution from silicon cascade transitions in the 4.43 MeV carbon peak can be calculated by multiplying $S_{Si1.78-GS,INS}$ (from Eq. (4)) and 0.0547. This contribution should be taken into account when determining the fraction of the 4.43 MeV peak that is due to carbon-12 in soil.

Contributions to the 4.43 MeV carbon peak by silicon cascade transitions can be determined from gamma spectrum measurements in the DC regime (i.e. at 100% duty cycle). In this case only one spectrum will be measured. In the DC regime the information regarding 1.78 MeV peak area due to decay of aluminum-28 produced by the ^{28}Si (n, p)^{28}Al reaction, and the decay of aluminum-28 produced by the $^{27}Al + n_{thermal} \rightarrow {}^{28}Al$ reaction with aluminum parts of equipment is unavailable. However, the fraction of the 4.50 MeV peak associated with silicon can be determined from measurement of silicon samples in the DC regime. Samples of granulated silicon (d = 1.26 g cm^{-3}; 40 cm × 40 cm area) at different thicknesses (1–20 cm) were used. All measurements were conducted at a height of 260 cm. Recorded spectra of silicon samples and NGA system background are shown in Fig. 11.

The peaks with centroid 1.78 MeV and 4.50 MeV in DC spectra of silicon samples and the NGA system background include all the same components as in the INS spectra. The differences between the 1.78 MeV and 4.50 MeV peak areas in the silicon sample and NGA system background spectra give the fraction of these peaks that are associated with silicon. The dependence of the 4.50 MeV

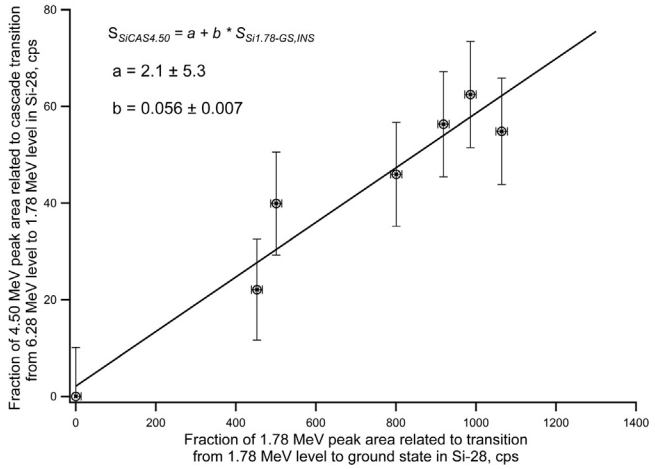

Fig. 10. The fraction of the peak area with energy 4.50 MeV related to cascade transition from 6.28 MeV level to 1.78 MeV level in silicon-28 versus the fraction of the peak area with energy 1.78 MeV related to transition from 1.78 MeV level to ground state in silicon-28.

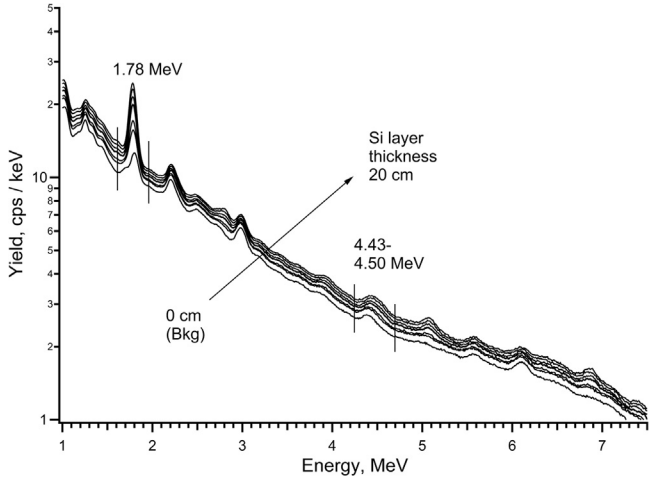

Fig. 11. DC spectra of the NGA system background and granulated silicon samples (d=1.26 g cm^{-3}) with an area of 40 cm × 40 cm with different layer thickness (1–20 cm) under 14 MeV neutron irradiation.

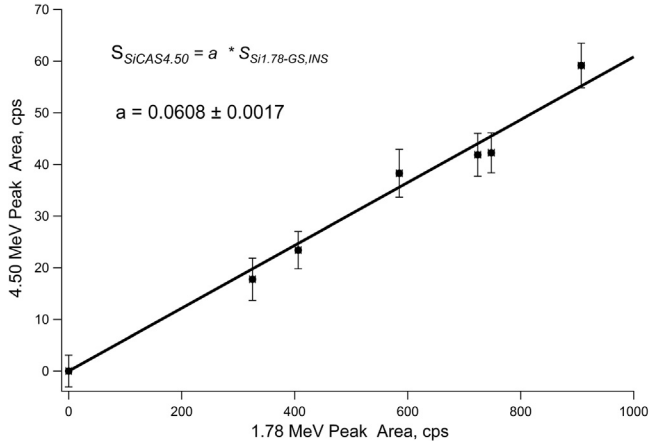

Fig. 12. Dependence of 4.43 MeV peak area with 1.78 MeV peak area in DC gamma spectra of granulated silicon irradiated by 14 MeV neutrons.

peak areas versus 1.78 MeV peak areas is shown in Fig. 12. As can be seen, this dependence can be fitted by a straight line passing through the origin with a slope of 0.0608. This coefficient can be used for determining the silicon fraction in the 4.43 MeV peak area for DC spectra of soil samples. The remaining portion of the 4.43 MeV peak area is caused by carbon-12 present in the soil.

3.3. System calibration

System calibration is important for understanding the dependence between carbon peak area in the neutron stimulated gamma-spectra and carbon in the soil sample. Several containers with mixtures of sand and granulated carbon (i.e., 1, 2.5, 5, 7.5, 10 and 15 *Cw%*) were analyzed at a 260 cm height. The acquired gamma spectra of these mixtures in the INS-TNC and DC regimes are shown in Fig. 13; enlarged regions of the INS and DC spectra near the 4.43 MeV carbon peak are also shown.

The fraction of the 4.43 MeV net peak associated with carbon ($S_{C4.43,INS}$ and $S_{C4.43,DC}$ in INS and DC spectra, respectively) can be calculated as follows:

$$S_{C4.43,INS} = S_{4.43,INS} - S_{Bkg4.43,INS} - S_{SiCAS4.43,INS} \quad (6)$$

$$S_{C4.43,DC} = S_{4.43,DC} - S_{Bkg4.43,DC} - S_{SiCAS4.43,DC} \quad (7)$$

where $S_{4.43,INS}$ and $S_{4.43,DC}$ are the 4.43 MeV peak areas in the INS and DC sample spectra (cps); $S_{Bkg4.43,INS}$ and $S_{Bkg4.43,DC}$ are the 4.43 MeV peak areas in the INS and DC background spectra (cps); and $S_{SiCAS4.43,INS}$ and $S_{SiCAS4.43,DC}$ are the part of the 4.43 MeV peak area related to cascade transitions from 6.28 to 1.78 MeV level in excited silicon-28 nuclei (cps).

Measurement live time (spectra acquisition) varies for the different measurements so all calculations (e.g., background subtraction, TNC spectra peak subtraction from corresponding INS spectra peaks, etc.) are executed in counts per second. In this case, $S_{SiCAS4.43,INS}$ and $S_{SiCAS4.43,DC}$ can be respectively defined as follows:

$$S_{SiCAS4.43,INS} = 0.0547 \times [(S_{1.78,INS} - S_{Bkg1.78,INS}) - (S_{1.78,TNC} - S_{Bkg1.78,TNC})] \quad (8)$$

$$S_{SiCAS4.43,DC} = 0.0608 \cdot (S_{1.78,DC} - S_{Bkg1.78,DC}) \quad (9)$$

where $S_{1.78,INS}$ and $S_{1.78,DC}$ are the 1.78 MeV peak areas in the sample spectra in the INS-TNC and DC regimes. Note that the previous equations and the coefficients 0.0547 and 0.0608 (INS and DC spectra, respectively) were based on the experimental direct proportional dependencies between the silicon fraction in the 4.43 and 1.78 MeV peaks for the both INS and DC spectra as discussed previously.

Based on the above described calculations, the dependencies between the corrected peak areas ($S_{C4.43,INS}$ and $S_{C4.43,DC}$; Eqs. (6), (7)) and carbon concentration in the mixtures were plotted and shown in Fig. 14 by points with error bars calculated by standard statistical equations (Gilmore, 2008). These dependencies can be fitted by a straight lines passing through the origin (Fig. 14). Thus, at a carbon concentration of 0%, the corrected peak areas for $S_{C4.43,INS}$ and $S_{C4.43,DC}$ should be equal to zero; this was observed with the sand measurement.

Slopes of the calibration lines are ~9.9 and 3.6 cps/*Cw%* for the INS-TNC and DC regimes, respectively. This slope difference is probably due to different neutron flux intensity during measurement live time. The total number of neutrons generated per pulse is the same for both regimes, but neutron flux is only generated during the duty cycle. In the INS regimes a 25% duty cycle was used while the DC regime had a 100% duty cycle. Therefore, the neutron flux intensity in the DC regime was approximately four

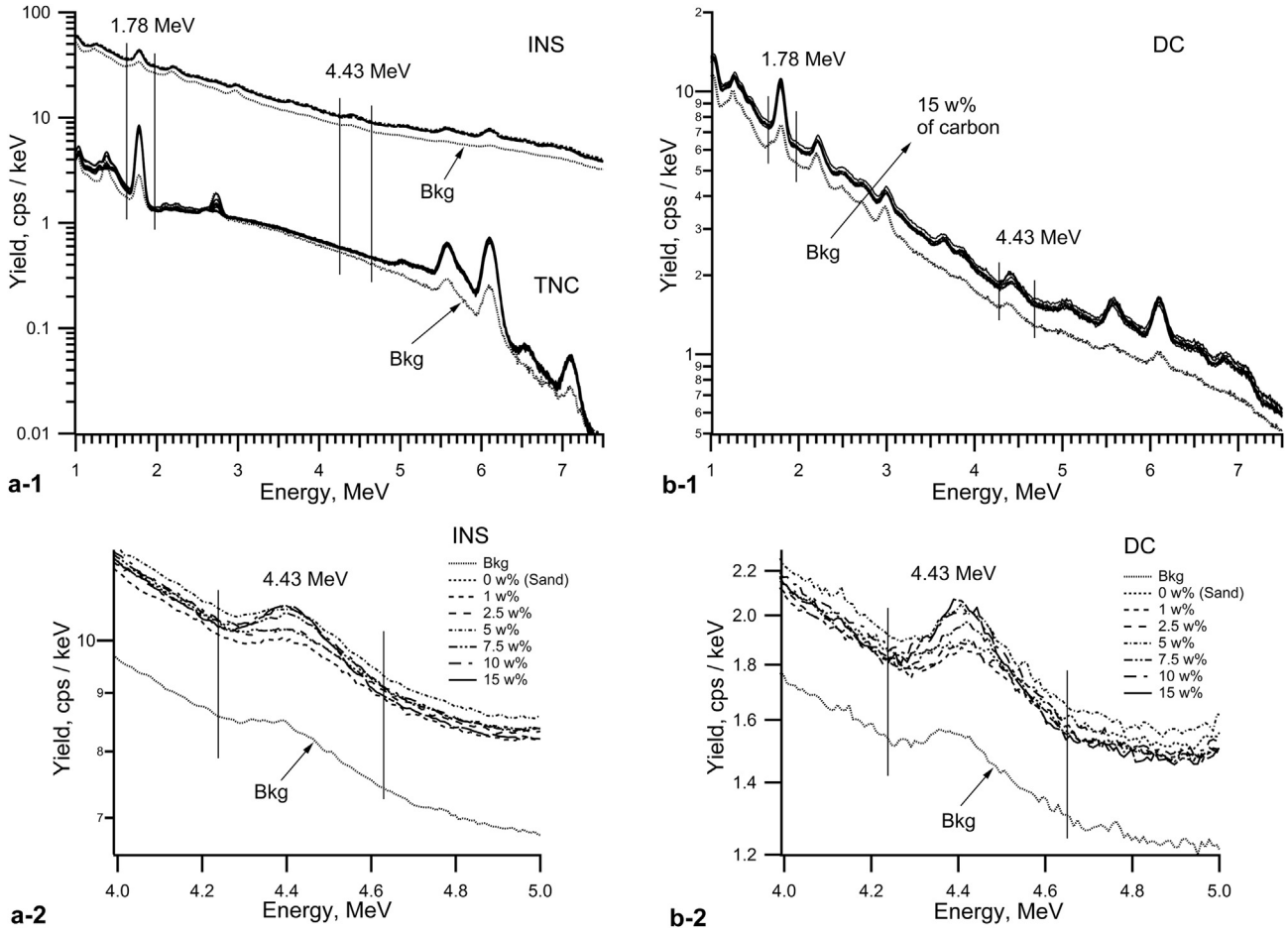

Fig. 13. INS-TNC (a-1) and DC (b-1) spectra of NGA system background and sand mixtures with 1–15 w% of granulated coconut shells under 14 MeV neutron irradiation, and fragments of INS (a-2) and DC (b-2) spectra around 4.43 MeV carbon peak in the enlarge scale. Sample volume was 40 cm × 40 cm × 20 cm. The regions of interest are shown in plots by vertical lines. All measurements were carried out at a height of 260 cm.

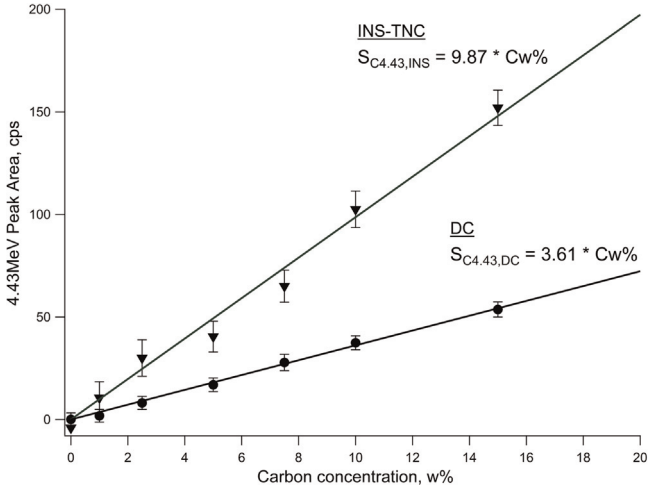

Fig. 14. The dependencies of a 4.43 MeV corrected peak areas for INS-TNC and DC regimes versus carbon content in sample (w%, points with error bars), and its straight lines approximation.

times less compared to INS-TNC. For INS, the higher neutron flux intensity also means that gamma ray flux is higher too, but detector dead time is also higher. This accounts for the count rate differences between INS and DC when measuring a sample with the same amount of carbon.

The average errors for $S_{C4.43,INS}$ and $S_{C4.43,DC}$ were approximately ± 8.1 and ± 3.4 cps, respectively; and errors of determination of carbon concentration are around ± 0.9 and ± 1.0 *Cw%* for INS-TNC and DC, respectively.

The DC measurement regime has some advantage over the INS-TNC regime. First of all, the DC measurement clock time was 30 min as opposed to 60 min for INS-TNC with approximately the same error for carbon concentration. In addition, the radioactive isotopes neutron source can be used for measurements in the continuous regime. Second, INS-TNC electronics (Tan et al., 2007; Mitra et al., 2007) are more complicated than those required for the continuous DC regime. Although the INS-TNC regime provides more information, the shorter sample time, simplicity of the DC set up, and methodology for handling data outlined in this manuscript indicates that the DC method is better suited for routine field measurements of soil carbon.

3.4. Measurements of carbon concentration in soil samples

Previously it was shown that the NGA system background, along with gamma signals contributed by silicon, should be accounted for when determining soil carbon using both the INS-TNC and DC regimes. Utilizing previously discussed methods, these regimes were used to experimentally determine the carbon concentration in soil samples with varying amounts of carbon to test the accuracy of the calibration.

Sample 1 shown in Table 1 was a Houston clay soil with a relatively high carbon concentration (i.e., ~2.8 w%) collected from

Table 1
Comparison of carbon measurements obtained by the NGA and dry combustion.

Sample number	Measurement mode	Measurement time (min)	Corrected carbon 4.43 MeV peak area ± error (cps)	Carbon concentration in sample ± error (w%)	
				NGA	Dry combustion method
1	DC	30	9.4 ± 3.4	2.8 ± 0.9	2.79 ± 0.13
	INS-TNC	60	27.9 ± 9.2	2.9 ± 1.0	
2	DC	30	24.8 ± 3.5	6.9 ± 1.0	7.76 ± 0.33
	INS-TNC	60	69.3 ± 7.7	7.1 ± 1.0	

an experimental soil bin at the National Soil Dynamics Laboratory. Sample 2 was a mixture of the same soil with an extra ~5 w% of added granulated carbon (coconut shells). Subsamples were collected from these and analyzed for carbon by the dry combustion method for comparison to NGA results.

Measured spectra were similar to spectra shown in Fig. 13. Calculations for corrected peak areas with centroids at 4.43 MeV for spectra produced by the INS-TNC and DC regimes were performed using Eqs. (8) and (9), respectively. Table 1 shows side-by-side comparison of soil carbon measurement to those obtained by the dry combustion method; similar soil carbon values were obtained using both methods. This data agreement suggests that with above described data processing, neutron-gamma analysis can feasibly be used to rapidly and accurately measure soil carbon in the field.

4. Conclusion

This work demonstrated the importance of accounting for system background caused by neutron interaction with the system components in data processing. With our current system configuration (i.e., 14 MeV neutron flux 10^8 s^{-1}; NaI (Tl) detector volume of ~2500 cm^3), this background can be measured at a distance of 250 cm above the ground and away from other structures. It was experimentally shown that neutron delay activation of aluminum construction components produces aluminum-28 nuclei and that their decay are responsible for the 1.78 MeV gamma peak in the background spectra. For both the DC and INS spectra, correction procedures were identified for removing system background and determining the portion of the 4.43 MeV peak area associated solely with carbon in samples. The ratio of 4.50–1.78 MeV peak areas due to a cascade transition of 6.28 MeV exited state level of silicon-28 to a ground state was experimentally determined to be 0.056 ± 0.007 and is in good agreement with the theoretical value of 0.0547. This value was used to calculate the portion of the 4.43 MeV peak area associated solely with carbon in the INS spectra.

This work identified correction procedures for determining the 4.43 MeV peak area due to carbon only (INS and DC spectra) which gave results that were directly proportional to the carbon concentration in soils samples (i.e., these dependencies passed through the zero–zero point origin). We estimate the minimum measurable soil carbon concentration to be ~1.5 *Cw%* (accuracy < ± 1 *Cw%*); increasing the number of detectors and measurement time may significantly improve this value.

The use of the continuous working regime (DC) significantly decreases measurement time compared to the pulse working regime while retaining the same degree of accuracy. Furthermore, a conventional multichannel gamma analyzer can be used in the continuous regime instead of the unique split electronics used in the pulse system. Thus, the continuous working regime (DC) is recommended for routine measurement of carbon concentration in soil.

Acknowledgment

The authors are indebted to Juan Rodriguez, Barry G. Dorman, Robert A. Icenogle, and Morris G. Welch for technical assistance in collecting and processing soil samples. The authors gratefully thank Dr. Sudeep Mitra for his invaluable advices during the implementation of this project. We thank XIA LLC for allowing the use of their electronics and detectors in this project.

References

Agostinelli, S., Allison, J., Amako, K., et al., 2003. Geant4-a simulation toolkit. Nucl. Inst. Methods A. 506, 250–303.
Basunia, M.S., 2013. Nuclear data sheets for A=28. Nucl. Data Sheets 114, 1189–1291.
Batchelor Jr., J.A., 1984. Properties of Bin Soils at the National Tillage Machinery Laboratory, Publication 218. USDA-ARS National Soil Dynamics Laboratory, Auburn, AL.
Geant4 10.0, 2014. Geant4 Software Download. ⟨http://geant4.web.cern.ch/geant4/support/download.shtml⟩.
Gilmore, G., 2008. Practical Gamma-Ray Spectrometry, second ed. John Wiley & Sons, LtD, West Sussex, England.
Gray, T., 2013. Isotope Abundance of the Elements. ⟨http://periodictable.com/Properties/A/IsotopeAbundances.html⟩.
Herman, M., Capote, R., Carlson, B.V., et al., 2007. EMPIRE: Nuclear reaction model code system for data evaluation. Nucl. Data Sheets 108, 2655–2715.
WaveMetrics, 2013. IGOR Pro. ⟨http://www.wavemetrics.com/products/igorpro/igorpro.htm⟩.
Kelley, K.R., 1994. Conveyor-belt apparatus for fine grinding of soil and plant materials. Soil Sci. Soc. Am. J. 58, 144–146.
MacFarlane, R.E., 2014. Interpreted ENDF file for sigma-ei. National Nuclear Data Center, Brookhaven National Laboratory, Upton NY.
Mitra, S., Wielopolski, L., Tan, H., et al., 2007. Concurrent measurement of individual gamma-ray spectra during and between fast neutron pulses. IEEE Trans. Nucl. Sci. 54 (1), 192–196.
Saint-Gobain Crystals, 2009. Efficiency Calculations for Selected Scintillators. ⟨http://www.crystals.saint-gobain.com/uploadedFiles/SG-Crystals/Documents/Technical/SGC%20Efficiency%20Calculations%20Brochure.pdf⟩.
Sonzogni, A., 2014. Chart of Nuclides. National Nuclear Data Center, Brookhaven National Laboratory, Upton NY.
Tan, H., Mitra, S., Wielopolski, L., et al., 2007. A digital spectrometer approach to obtaining multiple time-resolved gamma-ray spectra for pulsed spectroscopy. Nucl. Inst. Methods Phys. Res. B. 263, 63–66.
Turner, J.E., 2007. Atoms, Radiation, and Radiation Protection. Wiley-VCH Verlag GmbH & Co. KGaA, Weinheim, Germany.
Wielopolski, L., Mitra, S., Doron, O., 2008a. Non-carbon-based compact shadow shielding for 14 MeV neutrons. J. Radioanal. Nucl. Chem. 276 (1), 179–182.
Wielopolski, L., Hendrey, G., Johnsen, K.H., et al., 2008b. Nondestructive system for analyzing carbon in the soil. Soil Sci. Soc. Am. J. 72 (5), 1269–1277.
Wielopolski, L., 2011. Nuclear methodology for non-destructive multi-elemental analysis of large volumes of soil. In: Carayannis, E.G. (Ed.), Planet Earth 2011-Global Warming Challenges and Opportunities for Policy and Practice. InTech, Rijeka, Croatia, pp. 467–492.